

Synthesis and Properties of $\text{IrRe}_2(\mu\text{-H})_2(\text{CO})_9(\eta^5\text{-C}_9\text{H}_7)$

Matthew C. Comstock, Teresa Prussak-Wieckowska, Scott R. Wilson, and John R. Shapley*

School of Chemical Sciences, University of Illinois, Urbana, Illinois 61801

Received August 14, 1996[Ⓢ]

The slow addition of $\text{Re}_2(\mu\text{-H})_2(\text{CO})_8$ to a solution of $\text{Ir}(\text{CO})(\eta^2\text{-C}_8\text{H}_{14})(\eta^5\text{-C}_9\text{H}_7)$ in hexane at reflux provides $\text{IrRe}_2(\mu\text{-H})_2(\text{CO})_9(\eta^5\text{-C}_9\text{H}_7)$ (**1**) in 80% yield. The molecular structure of **1** shows an IrRe_2 triangle incorporating one $\text{Ir}(\text{CO})(\eta^5\text{-C}_9\text{H}_7)$ and two $\text{Re}(\text{CO})_4$ fragments. The strongly different Ir–Re distances suggest that one hydride ligand bridges one Ir–Re edge and the other hydride bridges the Re–Re edge. Low-temperature ^1H and ^{13}C NMR spectra are consistent with this structure; at higher temperatures a dynamic process involving migration of one hydride ligand between the two Ir–Re edges is observed. Cluster **1** is readily deprotonated with KOH/EtOH , and the resulting anion has been isolated as the PPN salt, $[\text{PPN}][\text{IrRe}_2(\mu\text{-H})(\text{CO})_9(\eta^5\text{-C}_9\text{H}_7)]$ (**2**). Both the ^1H and low temperature ^{13}C NMR spectra of **2** are consistent with a structure in which the remaining hydride ligand bridges the Re–Re edge. Variable-temperature ^{13}C NMR spectra indicate that **2** undergoes CO scrambling localized on the Ir–Re edges. The reaction of **1** with PPh_3 leads to $\text{IrRe}_2(\mu\text{-H})_2(\text{CO})_8(\text{PPh}_3)(\eta^5\text{-C}_9\text{H}_7)$ (**3**), which contains the phosphine on a rhenium atom, as well as to cluster fragmentation.

Introduction

The incorporation of indenyl-substituted metal fragments into metal clusters is a potential way to translate the enhanced reactivity of the “indenyl ligand effect”¹ from mononuclear compounds to polynuclear compounds. We recently reported that the reaction of $\text{Ir}(\text{CO})_2(\eta^5\text{-C}_9\text{H}_7)$ with $\text{Rh}(\eta^2\text{-C}_2\text{H}_4)_2(\eta^5\text{-C}_9\text{H}_7)$ led to formation of the trinuclear clusters $\text{Ir}_{3-x}\text{Rh}_x(\mu\text{-CO})_3(\eta^5\text{-C}_9\text{H}_7)_3$ ($x = 0\text{--}2$) in good yields,² and the compound $\text{Rh}_3(\mu\text{-CO})_3(\eta^5\text{-C}_9\text{H}_7)_3$ had been studied previously.³ These compounds react readily with carbon monoxide to form mononuclear products, whereas the corresponding cyclopentadienyl compounds are much less reactive. For example, $\text{Ir}_3(\mu\text{-CO})_3(\eta^5\text{-C}_9\text{H}_7)_3$ affords $\text{Ir}(\text{CO})_2(\eta^5\text{-C}_9\text{H}_7)$ quickly at room temperature, but $\text{Ir}_3(\text{CO})_3(\eta^5\text{-C}_5\text{H}_5)_3$ generates $\text{Ir}(\text{CO})_2(\eta^5\text{-C}_5\text{H}_5)$ only slowly in refluxing xylene (140 °C).⁴ Thus, indenyl ligand substitution does appear to enhance the reactivity of these clusters, but facile metal–metal bond scission precludes further cluster-based chemistry. We have been investigating routes toward other clusters containing indenyl ligands, and we now wish to report our results with the mixed-metal cluster, $\text{IrRe}_2(\mu\text{-H})_2(\text{CO})_9(\eta^5\text{-C}_9\text{H}_7)$ (**1**).

A general conceptual route to trinuclear clusters is the addition of mononuclear metal fragments to unsaturated $\text{M}=\text{M}$ species.⁵ Compounds of the form $\text{M}_2(\mu\text{-CO})_2(\eta^5\text{-L})_2$ ($\text{M} = \text{Co}, \text{Rh}, \text{Ir}; \text{L} = \text{C}_5\text{H}_5, \text{C}_5\text{Me}_5$) are well-established metal cluster synthons.⁶ The related unsaturated compound, $\text{Re}_2(\mu\text{-H})_2(\text{CO})_8$,⁷ has also shown some applications in cluster synthesis, leading to a variety

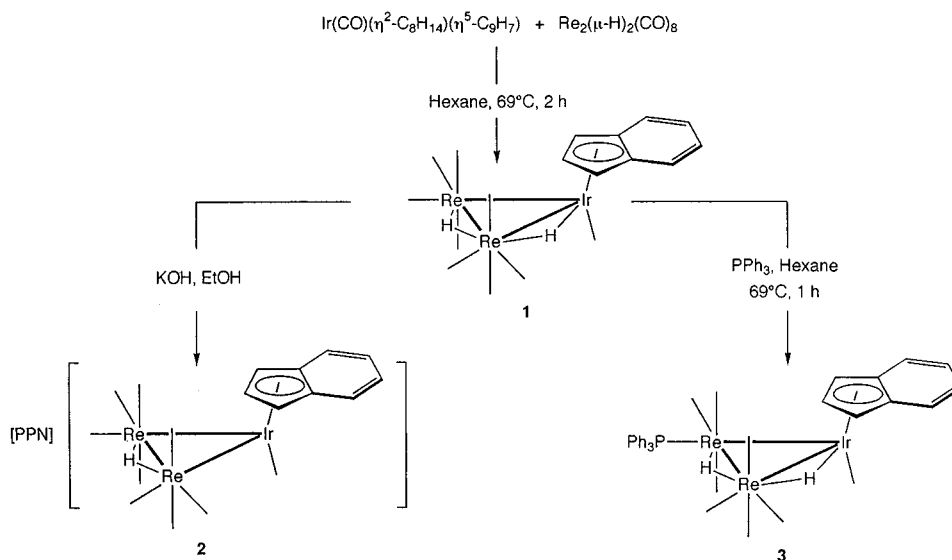
of PtRe_2 ^{8–10} as well as IrRe_2 ¹¹ mixed-metal clusters. For example, the reaction of $\text{Re}_2(\mu\text{-H})_2(\text{CO})_8$ with $\text{Pt}(\eta^4\text{-C}_8\text{H}_{12})_2$ provided the trinuclear cluster, $\text{PtRe}_2(\mu\text{-H})_2(\text{CO})_8(\eta^4\text{-C}_8\text{H}_{12})$.⁸ Reaction of the latter with 2 equiv of PPh_3 provided the compounds $\text{PtRe}_2(\mu\text{-H})_2(\text{CO})_8(\text{PPh}_3)_2$, which had been made previously from the reaction of $\text{Re}_2(\mu\text{-H})_2(\text{CO})_8$ with $\text{Pt}(\eta^2\text{-C}_2\text{H}_4)(\text{PPh}_3)_2$.⁹ Furthermore, the reaction of $\text{Re}_2(\mu\text{-H})_2(\text{CO})_8$ with $[\text{Ir}(\text{CO})_4]^-$ led to several clusters based on a IrRe_2 framework, such as $[\text{IrRe}_2\text{H}_2(\text{CO})_{11}]^-$, with a terminal hydride, and a hexanuclear cluster, $[\{\text{IrRe}_2(\mu\text{-H})(\text{CO})_{11}\}_2]^{2-}$, consisting of two IrRe_2 triangles joined by an Ir–Ir bond.¹¹ We now report that the reaction of $\text{Ir}(\text{CO})(\eta^2\text{-C}_8\text{H}_{14})(\eta^5\text{-C}_9\text{H}_7)$ ¹² with $\text{Re}_2(\mu\text{-H})_2(\text{CO})_8$ gives the trinuclear cluster $\text{IrRe}_2(\mu\text{-H})_2(\text{CO})_9(\eta^5\text{-C}_9\text{H}_7)$ (**1**), as shown in Scheme 1. Furthermore, deprotonation of **1** leads to $[\text{PPN}][\text{IrRe}_2(\mu\text{-H})(\text{CO})_9(\eta^5\text{-C}_9\text{H}_7)]$ (**2**), and the reaction

- (6) (a) Adams, R. D. In *Comprehensive Organometallic Chemistry II*; Abel, E. W., Stone, F. G. A., Wilkinson, G., Eds.; Pergamon: New York, 1995; Vol. 10, Chapter 1, pp 6, 7. (b) Barnes, C. E. In *Comprehensive Organometallic Chemistry II*; Abel, E. W., Stone, F. G. A., Wilkinson, G., Eds.; Pergamon: New York, 1995; Vol. 8, Chapter 4, pp 429–431, 512. (c) Adams, R. D. In *The Chemistry of Metal Cluster Complexes*; Shriver, D. F., Kaesz, H. D., Adams, R. D., Eds.; VCH: New York, 1990; Chapter 3, pp 153–158. (d) Barr, R. D.; Green, M.; Howard, J. A. K.; Marder, T. B.; Stone, F. G. A. *J. Chem. Soc., Chem. Commun.* **1983**, 759. (e) Barr, R. D.; Green, M.; Howard, J. A. K.; Marder, T. B.; Orpen, A. G.; Stone, F. G. A. *J. Chem. Soc., Dalton Trans.* **1984**, 2757. (f) Barr, R. D.; Green, M.; Marsden, K.; Stone, F. G. A.; Woodward, P. *J. Chem. Soc., Dalton Trans.* **1983**, 507. (g) Barnes, C. E.; Dial, M. R.; Orvis, J. A.; Staley, D. L.; Rheingold, A. L. *Organometallics* **1990**, 9, 1021. (h) Barnes, C. E.; Dial, M. R. *Organometallics* **1988**, 7, 782.
- (7) Bennett, M. J.; Graham, W. A. G.; Hoyano, J. K.; Hutcheon, W. L. *J. Am. Chem. Soc.* **1972**, 94, 6232.
- (8) (a) Ciani, G.; Moret, M.; Sironi, A.; Antognazza, P.; Beringhelli, T.; D'Alfonso, G.; Della Pergola, R.; Minoja, A. *J. Chem. Soc., Chem. Commun.* **1991**, 1255. (b) Antognazza, P.; Beringhelli, T.; D'Alfonso, G.; Minoja, A.; Ciani, G.; Moret, M.; Sironi, A. *Organometallics* **1992**, 11, 1777.
- (9) (a) Beringhelli, T.; Ceriotti, A.; D'Alfonso, G.; Della Pergola, R.; Ciani, G.; Moret, M.; Sironi, A. *Organometallics* **1990**, 9, 1053. (b) Beringhelli, T.; D'Alfonso, G.; Minoja, A. P. *Organometallics* **1991**, 10, 394.
- (10) Xiao, J.; Puddephatt, R. J. *Coord. Chem. Rev.* **1995**, 143, 457.
- (11) Beringhelli, T.; Ciani, G.; D'Alfonso, G.; Garlaschelli, L.; Moret, M.; Sironi, A. *J. Chem. Soc., Dalton Trans.* **1992**, 1865.
- (12) (a) Szajek, L. P.; Lawson, R. J.; Shapley, J. R. *Organometallics* **1991**, 10, 357. (b) Szajek, L. P.; Shapley, J. R. *Organometallics* **1994**, 13, 1395.

[Ⓢ] Abstract published in *Advance ACS Abstracts*, September 1, 1997.

- (1) (a) Ji, L.-N.; Rerek, M. E.; Basolo, F. *Organometallics* **1984**, 3, 740. (b) Rerek, M. E.; Basolo, F. *J. Am. Chem. Soc.* **1984**, 106, 5908. (c) Kakkar, A. K.; Taylor, N. J.; Marder, T. B.; Shen, J. K.; Hallinan, N.; Basolo, F. *Inorg. Chim. Acta* **1992**, 198–200, 219.
- (2) Comstock, M. C.; Wilson, S. R.; Shapley, J. R. *Organometallics* **1994**, 13, 3805.
- (3) (a) Caddy, P.; Green, M.; O'Brien, E.; Smart, L. E.; Woodward, P. *Angew. Chem., Int. Ed. Engl.* **1977**, 16, 648; *Angew. Chem.* **1977**, 89, 671. (b) Al-Obaidi, Y. N.; Green, M.; White, N. D.; Taylor, G. E. *J. Chem. Soc., Dalton Trans.* **1982**, 319.
- (4) Shapley, J. R.; Adair, P. C.; Lawson, R. J.; Pierpont, C. G. *Inorg. Chem.* **1982**, 21, 1701.
- (5) (a) Hoffmann, R. *Angew. Chem., Int. Ed. Engl.* **1982**, 21, 711; *Angew. Chem.* **1982**, 94, 725. (b) Stone, F. G. A. *Angew. Chem., Int. Ed. Engl.* **1984**, 23, 89; *Angew. Chem.* **1984**, 96, 85.

Scheme 1



of **1** with PPh_3 provides both $\text{IrRe}_2(\mu\text{-H})_2(\text{CO})_8(\text{PPh}_3)(\eta^5\text{-C}_9\text{H}_7)$ (**3**) as well as considerable cluster fragmentation.

Experimental Section

General Procedures. All reactions were conducted under an atmosphere of nitrogen with use of standard Schlenk techniques. $\text{Ir}(\text{CO})(\eta^2\text{-C}_8\text{H}_{14})(\eta^5\text{-C}_9\text{H}_7)$ was prepared by the literature method.¹² $\text{Re}_2(\mu\text{-H})_2(\text{CO})_8$ was prepared by a modification of the literature procedure;¹³ using benzene rather than hexane led to a higher yield (62% vs 35%). Solvents for preparative use were dried by standard methods and distilled prior to use. Deuterated solvents for NMR studies, $(\text{CD}_3)_2\text{CO}$ and CD_2Cl_2 (Cambridge Isotope Laboratories), were used as received.

Proton NMR spectra were recorded on General Electric QE-300 or GN300NB spectrometers and were referenced to residual solvent resonances (δ 2.04 for acetone- d_5 and δ 5.32 for CH_2Cl_2). Carbon-13 NMR spectra were recorded on General Electric GN300NB (at 75 MHz), GN500 (at 125 MHz) or Varian U400 (at 100 MHz) spectrometers and were referenced to solvent resonances (δ 29.8 ($\text{CD}_3)_2\text{CO}$ or δ 53.8 for CD_2Cl_2). Phosphorus-31 spectra were recorded at 121.6 MHz on a General Electric GN-300NB spectrometer and referenced to external 85% H_3PO_4 . Infrared spectra were recorded on a Perkin-Elmer 1750 FT spectrophotometer. Mass spectra were recorded on either a Finnigan-Mat 731 spectrometer (field desorption, FD) or a VG ZAB-SE spectrometer (fast atom bombardment, FAB) by the staff of the Mass Spectrometry Laboratory of the School of Chemical Sciences. Microanalyses were performed by the staff of the School Microanalytical Laboratory.

The ^1H - ^{13}C correlation spectrum (HETCOR) of **1** was recorded on a GN500 spectrometer. A total of 48 transients of 2k data points were recorded for each of the 128 increments of t_1 (spectral width in $F_2 = 4808$ Hz, spectral width in $F_1 = 5291$ Hz, relaxation delay = 1 s). The spectrum was optimized for $^2J_{\text{CH}} = 10$ Hz.

$\text{IrRe}_2(\mu\text{-H})_2(\text{CO})_9(\eta^5\text{-C}_9\text{H}_7)$ (1**).** A solution of $\text{Ir}(\text{CO})(\eta^2\text{-C}_8\text{H}_{14})(\eta^5\text{-C}_9\text{H}_7)$ (51.3 mg, 0.115 mmol) in hexane (5 mL) was stirred and heated at reflux, and then a benzene solution (20 mL) of $\text{Re}_2(\mu\text{-H})_2(\text{CO})_8$ (138 mg, 0.231 mmol) was added slowly through an addition funnel over 90 min. The mixture was heated at reflux for an additional 30 min, resulting in a dark orange solution. The solvent was removed under vacuum, and the residue was extracted with hexane (6×10 mL) through a filter cannula. The tan residue remaining in the reaction flask was largely $\text{Re}_3(\mu\text{-H})_3(\text{CO})_{12}$, identified by its infrared peaks in hexane at 2094 m, 2032 s, 2009 s, 1984 cm^{-1} (lit.¹⁴ (cyclohexane):

2093 m, 2030 s, 2008 s, 1983 cm^{-1}). The extracts were dried on a rotary evaporator, and the orange residue was redissolved in CH_2Cl_2 . A small amount of neutral alumina I (Aldrich) was added, and the mixture was dried under vacuum, and then placed on a 15 cm \times 1 cm column of neutral alumina I. Elution with Et_2O removed a yellow fraction that contained unreacted $\text{Ir}(\text{CO})(\eta^2\text{-C}_8\text{H}_{14})(\eta^5\text{-C}_9\text{H}_7)$, identified by infrared spectroscopy.¹² Elution with CH_2Cl_2 removed an orange band that was dried under vacuum to give orange, crystalline **1**. Yield: 86 mg (0.092 mmol, 80% based on Ir). IR (ν_{CO} , hexane): 2104 m, 2076 m, 2013 s, 2000 m, 1988 sh, 1982 m, 1969 m, 1945 cm^{-1} . Anal. Calcd for $\text{C}_{18}\text{H}_9\text{O}_9\text{IrRe}_2$: C, 23.15; H, 0.97. Found: C, 23.17; H, 0.96. FD-MS (100 °C): m/z (^{193}Ir , ^{187}Re) 936, $\text{IrRe}_2\text{H}_2(\text{CO})_9(\text{C}_9\text{H}_7)^+$.

[PPN][$\text{IrRe}_2(\mu\text{-H})(\text{CO})_9(\eta^5\text{-C}_9\text{H}_7)$] (2**).** A yellow solution of **1** (40 mg 0.042 mmol) in ethanol was treated with KOH in ethanol (2.2 mL, 0.021 M, 0.046 mmol). The color changed immediately to deep red. A solution of [PPN][Cl] (243 mg, 0.424 mmol) in ethanol (5 mL) was added via cannula, the volume was reduced to ca. 5 mL under vacuum, and the mixture was held at -20 °C for 12 h. The red needles that precipitated were washed with ethanol at 0 °C (6×5 mL) and Et_2O (4×5 mL) and dried under vacuum. Yield: 31 mg (0.021 mmol, 50%). IR (ν_{CO} , EtOH): 2065 m, 2033 m, 1970 s, 1946 m, 1906 cm^{-1} . Anal. Calcd for $\text{C}_{34}\text{H}_{38}\text{IrNO}_9\text{P}_2\text{Re}_2$: C, 44.08; H, 2.60; N, 0.95. Found: C, 44.34; H, 2.89; N, 1.12. FAB(-)-MS (25 °C): m/z (^{193}Ir , ^{187}Re) 935, $\text{IrRe}_2\text{H}(\text{CO})_9(\text{C}_9\text{H}_7)^+$.

Reaction of **1 with PPh_3 .** A hexane solution (15 mL) of **1** (52.9 mg, 0.0566 mmol) and PPh_3 (16.3 mg, 0.062 mmol) was stirred and heated at reflux for 1 h. The infrared spectrum of the resulting solution showed the presence of remaining **1** as well as peaks for $\text{ReH}(\text{CO})_4(\text{PPh}_3)$ at 2081, 1993, 1977, and 1964 cm^{-1} (lit.¹⁵ (hexane): 2079, 1992, 1976, 1963 cm^{-1}). The mixture was placed directly on a 15 cm \times 1 cm column of neutral alumina. Elution with hexane/dichloromethane (8:1) removed an orange band containing **1** (18 mg, 0.019 mmol, 34% recovery). Elution with hexane/dichloromethane (1:1) removed a second orange band, which was dried under vacuum and further purified by preparative TLC (silica gel, hexane/ Et_2O , 9:1) to give **3** (11.3 mg, 0.010 mmol, 17%). Anal. Calcd for $\text{C}_{35}\text{H}_{24}\text{IrO}_8\text{PRe}_2$: C, 35.99; H, 2.07. Found: C, 36.04; H, 2.03. IR (ν_{CO} , hexane): 2079 m, 2044 w, 2022 w, 1994 s, 1974 m, 1967 m, 1934 cm^{-1} . FD-MS (100 °C): m/z (^{193}Ir , ^{187}Re) 1170, $\text{IrRe}_2\text{H}_2(\text{CO})_8(\text{PPh}_3)(\text{C}_9\text{H}_7)^+$; 1142, $\text{IrRe}_2\text{H}(\text{CO})_7(\text{PPh}_3)(\text{C}_9\text{H}_7)^+$; 880, $\text{IrRe}_2\text{H}_2(\text{CO})_7(\text{C}_9\text{H}_7)^+$.

X-ray Crystal Structure Study of **1.** The orange, tabular crystal was mounted using oil (Paratone-N, Exxon) to a thin glass fiber. Data were measured at 198 K on an Enraf-Nonius CAD4 diffractometer. Crystal and refinement details are given in Table 1. Systematic conditions suggested the space group $P\bar{1}$; refinement confirmed the

(13) Andrews, M. A.; Kirtley, S. W.; Kaesz, H. D. *Inorg. Chem.* **1977**, *16*, 1556.

(14) Huggins, D. K.; Fellman, W.; Smith, J. M.; Kaesz, H. D. *J. Am. Chem. Soc.* **1964**, *86*, 4841.

(15) Flitcroft, N.; Leach, J. M.; Hopton, F. J. *J. Inorg. Nucl. Chem.* **1970**, *32*, 137.

Table 1. Crystallographic Data for IrRe₂(μ-H)₂(CO)₉(η⁵-C₉H₇)

formula	C ₁₈ H ₉ IrO ₉ Re ₂	fw	933.85
space group, system	P1, triclinic	temp	198(2) K
a	8.618(4) Å	λ	0.710 73 Å (Mo Kα)
b	9.430(2) Å	ρ _{calcd}	2.981 g cm ⁻³
c	14.729(4) Å	I _{tot} (unique, R _i)	3120 (2894, 0.0283)
α	81.52(2)°	μ	18.032 mm ⁻¹
β	74.97(3)°	max/min trans	0.368/0.128
γ	64.25(3)°	goodness of fit (F ²) ^a	1.149
V	1040.4(6) Å ³	R1, ^b wR2 [I > 2σ(I)] ^c	0.0277, 0.0681
Z	2	R1, ^b wR2 (all data) ^c	0.0388, 0.0812

^a GOF = [Σ[w(F_o² - F_c²)²]/(n - p)]^{1/2}; n = number of reflections, p = total number of parameters refined. ^b R1 = Σ||F_o - |F_c||/Σ|F_o|. ^c wR2 = [Σ[w(F_o² - F_c²)²]/Σ[w(F_o²)]^{1/2}.

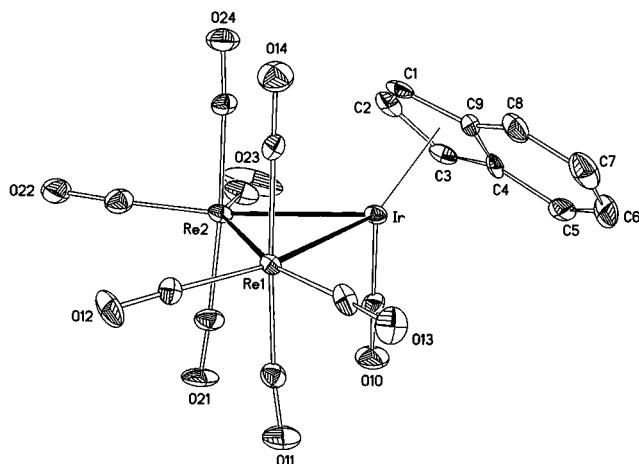
Table 2. Selected Structural Data for IrRe₂(μ-H)₂(CO)₉(η⁵-C₉H₇)

Internuclear Distances			
Ir-Re1	3.020(1)	Re1-C11	1.98(1)
Ir-Re2	2.866(1)	Re1-C12	1.95(1)
Re1-Re2	3.095(2)	Re1-C13	1.94(1)
Ir1-C1	2.26(1)	Re1-C14	1.98(1)
Ir1-C2	2.23(1)	Re2-C21	2.01(1)
Ir1-C3	2.18(1)	Re2-C22	1.88(1)
Ir1-C4	2.35(1)	Re2-C23	1.94(1)
Ir1-C9	2.39(1)	Re2-C24	1.98(1)
Ir1-C10	1.81(1)		
Bond Angles			
Ir-Re1-Re2	55.87(3)	C11-Re1-C14	177.2(5)
Ir-Re1-C11	90.2(3)	C23-Re2-C22	93.1(6)
Ir-Re1-C12	164.0(3)	C21-Re2-C24	176.2(5)
Ir-Re1-C13	103.9(3)	Ir-Re2-Re1	60.73(3)
Ir-Re1-C14	87.6(3)	Ir-Re2-C21	98.6(4)
C11-Re1-Re2	88.0(3)	Ir-Re2-C22	170.9(4)
C12-Re1-Re2	108.2(3)	Ir-Re2-C23	92.0(4)
C13-Re1-Re2	159.5(3)	Ir-Re2-C24	85.1(3)
C14-Re1-Re2	92.0(4)	C21-Re2-Re1	89.2(4)
Re2-Ir-Re1	63.40(3)	C22-Re2-Re1	114.6(4)
Re1-Ir-C10	95.2(4)	C23-Re2-Re1	152.2(4)
Re2-Ir-C10	84.9(4)	C24-Re2-Re1	91.7(3)
C13-Re1-C12	92.1(4)		

presence of a symmetry center. Step-scanned intensity data were reduced by profile analysis¹⁶ and corrected for Lorentz-polarization effects and for absorption.¹⁷ Scattering factors and anomalous dispersion terms were taken from standard tables.¹⁸ The structure of **1** was solved by direct methods;¹⁹ correct positions for the metal atoms were deduced from an E-map. One cycle of isotropic least-squares refinement followed by an unweighted difference Fourier synthesis revealed positions for the remaining non-H atoms. Bridging hydrogens never surfaced in the difference Fourier maps; the remaining hydrogen atoms were included as fixed idealized contributors. Non-H atoms were refined with anisotropic thermal coefficients. Successful convergence of the full-matrix least-squares refinement of F² was indicated by the maximum shift/error for the last cycle.²⁰ The highest peaks in the final difference Fourier map were in the vicinity of the metal atoms; the final map had no other significant features. Selected structural data for **1** are given in Table 2.

Results and Discussion

Synthesis and Characterization of 1. The slow addition of Re₂(μ-H)₂(CO)₈ to Ir(CO)(η⁵-C₈H₁₄)(η⁵-C₉H₇) in refluxing hexane forms the heterometallic cluster IrRe₂(μ-H)₂(CO)₉(η⁵-C₉H₇), **1**, in high yield (80% isolated). In contrast, heating a

**Figure 1.** ORTEP diagram of the molecular structure of **1** (35% probability ellipsoids).

mixture of Re₂(μ-H)₂(CO)₈ and Ir(CO)(η⁵-C₈H₁₄)(η⁵-C₉H₇) in hexane for the same amount of time leads to lower yields of **1**, recovery of significant amounts of Ir(CO)(η⁵-C₈H₁₄)(η⁵-C₉H₇), and the formation of large amounts of Re₃(μ-H)₃(CO)₁₂. The difference apparently relates to the effective lifetime of the reactive dirhenium species, since it has been observed that heating a solution of Re₂(μ-H)₂(CO)₈ in hexane at reflux produces Re₃(μ-H)₃(CO)₁₂.²¹ The mass spectrum of **1** is consistent with the proposed formula, and the IR spectrum in hexane shows several terminal carbonyl stretching bands. The ¹H NMR spectrum contains two peaks in the hydride region and one set of indenyl resonances. Further NMR spectroscopic studies of **1** are discussed below.

Molecular Structure of 1. The significant structural results from the X-ray diffraction study of **1** are summarized in Table 2, and a diagram of the molecule is shown in Figure 1. The cluster consists of an IrRe₂ triangle incorporating one Ir(CO)(η⁵-C₉H₇) and two Re(CO)₄ fragments. Within the metal triangle, Ir-Re1 = 3.020(1), Ir-Re2 = 2.866(1), and Re1-Re2 = 3.095(2) Å. The hydride ligands were not located explicitly, but one presumably bridges the long Ir-Re edge and one occupies the Re-Re edge. A similar explanation was offered to explain the two different Pt-Re distances in PtRe₂(μ-H)₂(CO)₈(η⁴-C₈H₁₂)⁸ and in PtRe₂(μ-H)₂(CO)₈(PPh₃)₂.⁹ In the former, the two Pt-Re distances are 2.895(1) and 2.741(1) Å and the Re-Re distance is 3.115(1) Å. In the latter, the two Pt-Re distances are 2.906(1) and 2.788(1) Å and the Re-Re distance is 3.203(1) Å.⁹ Furthermore, in **1** and in these PtRe₂ clusters, the Re-Re distances are longer than that in Re₂(CO)₁₀ (3.02 Å)²² and are comparable with the Re(μ-H)Re distances in Re₃(μ-H)₃(CO)₁₂ (3.241(2) Å)²¹ and [Re₃(μ-H)₂(CO)₁₂]⁻

(16) Coppins, P.; Blessing, R. H.; Becker, P. *J. Appl. Crystallogr.* **1972**, 7, 488.

(17) Sheldrick, G. M. SHELX-76. Program for crystal structure determination, Univ. of Cambridge, England, 1976.

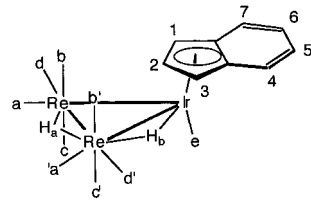
(18) Wilson, A. J. C., Ed. *International Tables for X-ray Crystallography*; Kluwer Academic Publishers: Dordrecht, The Netherlands, 1992; Vol. C: (a) scattering factors, pp 500-502; (b) anomalous dispersion corrections, pp 219-222.

(19) Sheldrick, G. M. SHELXS-86. *Acta Crystallogr.* **1990**, A46, 467.

(20) Sheldrick, G. M. SHELXL-93, University of Göttingen, 1993.

(21) Masciocchi, N.; Sironi, A.; D'Alfonso, G. *J. Am. Chem. Soc.* **1990**, 112, 9395.

(22) Dahl, L. F.; Ishishi, E.; Rundle, R. E. *J. Chem. Phys.* **1957**, 26, 1750.

Table 3. Proton and Carbon NMR Data for Compounds **1–3**^a


cmpd	¹ H chem shifts						Re/Ir carbonyl ¹³ C chem shifts				
	H ₂	H _{1, H3} ^b	H _{4, H7} ^b	H _{5, H6} ^b	H _a	H _b	a, a'	b, b' ^c	c, c' ^c	d, d'	e
1 ^d	6.80	6.71, 5.63	7.90, 7.59	7.44–7.51	–16.42	–17.56	191.2, 187.1	190.3, 182.9 ^e	185.9, 182.9 ^e	182.5, 179.5	168.4
2 ^f	5.64 ^g	5.55 ^g	7.38	6.94		–17.75	189.5 ^h	197.3 ^h	196.3 ^h	184.1	174.6
3 ⁱ	6.27	6.22, 5.56	7.69–7.27 ^j	7.69–7.27 ^j	–15.19 ^k	–17.12	(P), ^l 192.0	193.1, ^m 191.3	189.2, ^m 187.1	187.9, ^m 183.1	168.4

^a The labeling scheme shown above was used for assignments of the resonances of **1**, **2**, and **3**. ^b Specific assignments of related protons, e.g., H₁, H₃, are not determined for **1** and **3**. ^c For both **1** and **2**, the assignments of the b and c sets of resonances are interchangeable. ^d In acetone-*d*₆ at –70 °C. For the chemical shifts for selected nuclei in CD₂Cl₂ at –80 °C see Figure 4. ^e This resonance has an intensity corresponding to 2C. ^f In CD₂Cl₂; ¹H data at 25 °C and ¹³C data at –60 °C. ^g *J*₁₂ = *J*₂₃ = 2.6 Hz. ^h The uncoupled ¹³C spectrum of **2** at –60 °C showed these three peaks as doublets with *J*_{HC} = 2.7 (b), 3.0 (c), and 4.0 (a) Hz. ⁱ In CD₂Cl₂ at 25 °C. ^j The resonances for H₄–H₇ overlap with those for the phenyl protons on PPh₃. ^k *J*_{PH₃} = 16.4 Hz. ^l Assumed position of the PPh₃ ligand; see text and I. ^m These three peaks appear as doublets with *J*_{PC} = 6.6 (b), 7.9 (c), and 8.2 (d) Hz.

(3.173(7) and 3.181(7) Å).²³ The unbridged Re–Re distance in the latter complex ion is 3.035(7) Å.²³

The Ir–Re distance of Ir–Re2 = 2.866(1) in **1** may be compared with other examples of unsupported Ir–Re bonds. The closed Re₂Ir cluster Re₂(CO)₈(μ-PCy₂)(μ-Ir(CO)₂PPh₃) shows an average distance of Ir–Re = 2.962(1) Å.²⁴ The average Ir–Re distances are 2.879 Å in the iridium-capped, carbido cluster, [Re₇C(CO)₂₁Ir(η²-C₂H₄)(CO)]^{2–},²⁵ and 2.914(1) Å in the linear compound, {Re(CO)₅}₂IrH(CO)₃.²⁶ The cluster [IrRe₃(μ-H)(CO)₁₆][–] has an average Ir–Re distance of 2.93 Å within the IrRe₂ triangle and a distance of 2.935 Å for the spike Ir–Re bond.¹¹ The dinuclear compound, IrRe(μ-CO)₂(CO)₂(η⁵-C₅H₅)(η⁵-C₅Me₅), containing semi-bridging CO ligands, has an Ir–Re distance of 2.8081(6) Å.²⁷

As pointed out initially in studies by Churchill, e.g. in [Re₃(μ-H)₂(CO)₁₂][–]²³ and Os₃H(μ-H)(CO)₁₁,²⁸ the arrangement of the equatorial carbonyl ligands provide further insight into the location of bridging hydride ligands. In the structure of **1**, the Ir–Re2–C23 angle of 92.1(4)° is small compared to the Ir–Re1–C13 angle of 103.9(3)°, consistent with the position of a hydride ligand along the Ir–Re1 edge that forces an expanded angle. Furthermore, both the C22–Re2–Re1 angle of 114.6(4)° and the C12–Re1–Re2 angle of 108.2(3)° are relatively large, again consistent with the presence of a bridging hydride ligand on the Re1–Re2 edge. All of the axial carbonyl ligands are nearly orthogonal to the IrRe₂ plane.

The mean plane of the indenyl ligand five carbon ring makes an angle of 46.5(2)° with respect to the IrRe₂ plane. The structural details of indenyl ligand bonding in M(η⁵-C₉H₇) compounds can be described by the slip distortion parameter (Δ), the fold angle, and the hinge angle.²⁹ In compound **1**, Δ

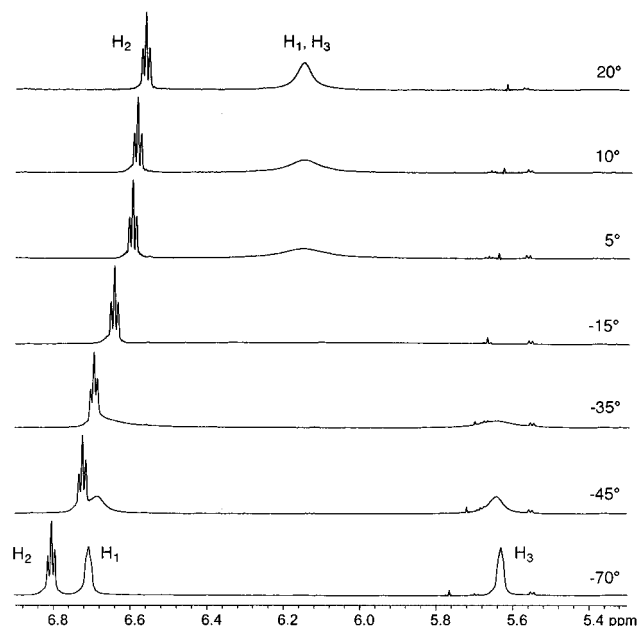


Figure 2. Proton NMR spectra of **1** in acetone-*d*₆ at temperatures from 20 to –70 °C, showing the indenyl H₁–H₃ region.

= 0.15 Å, the fold angle = 6.6(1.3)°, and the hinge angle = 7.5(1.4)°. These values imply a distortion slightly less than that for C_{3v}-Ir₃(μ₃-CO)₃(η⁵-C₉H₇)₃,² which has average values for the three indenyl ligands of Δ = 0.27 Å, fold angle = 10.1°, and hinge angle = 9.5°. However, the corresponding values in [Ir₃{Au(PPh₃)₃}(CO)₃(η⁵-C₉H₇)₃]⁺³⁰ are Δ = 0.11 Å, fold angle = 9.1°, and hinge angle = 6.2°, and in the mononuclear compound Ir(CO)(η²-C₂H₂(CO₂Me)₂)(η⁵-C₉H₇)³¹ are Δ = 0.17 Å, fold angle = 6.0°, and hinge angle = 7.4°. Thus, the indenyl ligand in **1** shows no unusual structural features.

Solution NMR spectroscopic studies of 1. At low temperatures both the ¹H and ¹³C NMR spectra of **1** (see Table 3 and Figures 2 and 3) are consistent with the solid-state structure of the molecule. In particular, the H₁ and H₃ protons of the indenyl ligand are inequivalent, which indicates that the ligand occupies an asymmetric site, and two hydride resonances are observed. The ¹³C{¹H} NMR spectrum in acetone-*d*₆ shows seven singlets

(23) Churchill, M. R.; Bird, P. H.; Kaesz, H. D.; Bau, R.; Fontal, B. *J. Am. Chem. Soc.* **1968**, *90*, 7135.

(24) Haupt, H.-J.; Flörke, U.; Beckers, H.-G. *Inorg. Chem.* **1994**, *33*, 3481.

(25) Ma, L.; Wilson, S. R.; Shapley, J. R. *Inorg. Chem.* **1990**, *29*, 5133.

(26) Breimair, J.; Robl, C.; Beck, W. *J. Organomet. Chem.* **1991**, *411*, 395.

(27) Zhuang, J.-M.; Batchelor, R. J.; Einstein, F. W. B.; Jones, R. H.; Hader, R.; Sutton, D. *Organometallics* **1990**, *9*, 2723.

(28) Shapley, J. R.; Keister, J. B.; Churchill, M. R.; DeBoer, B. G. *J. Am. Chem. Soc.* **1975**, *97*, 4145.

(29) (a) Faller, J. W.; Crabtree, R. H.; Habib, A. *Organometallics* **1985**, *4*, 929. (b) Baker, R. T.; Tulip, T. H. *Organometallics* **1986**, *5*, 839. (c) Donovan, B. T.; Hughes, R. P.; Trujillo, H. A.; Rheingold, A. L. *Organometallics* **1992**, *11*, 64. (d) Kakkar, A. K.; Taylor, N. J.; Calabrese, J. C.; Nugent, W. A.; Roe, D. C.; Connaway, E. A.; Marder, T. B. *J. Chem. Soc., Chem. Commun.* **1989**, 990.

(30) Comstock, M. C.; Prussak-Wieckowska, T.; Wilson, S. R.; Shapley, J. R. *Organometallics*, in press.

(31) Du, Y.; Wilson, S. R.; Shapley, J. R. Unpublished results.

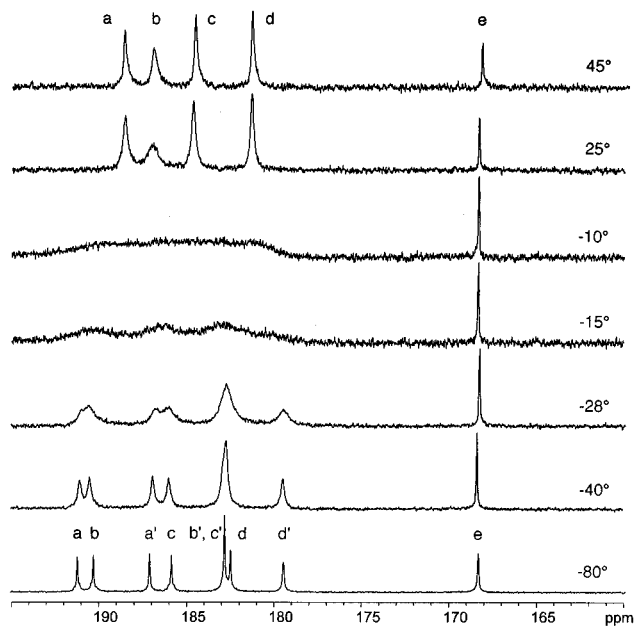


Figure 3. Carbon-13 NMR spectra (carbonyl region) of **1** in acetone-*d*₆ at temperatures between 45 and -80 °C.

between 192 and 179 ppm due to the eight carbonyls on the Re atoms (two resonances are overlapped) and one singlet at δ 168.4 for the CO ligand on the iridium atom (see Figure 3, bottom spectrum). The latter assignment is based on further observations discussed below and on comparison with the resonances for the CO ligands in Ir(CO)(η^2 -C₂H₄)(η^5 -L), which appear at δ 169.9 and 168.3 for L = C₅H₅ and C₉H₇, respectively,¹² and in the iridium-capped cluster, [Re₇C(CO)₂₁-Ir(η^2 -C₈H₁₄)(CO)]²⁻, which has a peak at δ 167.1 assigned to the Ir-CO ligand.²⁵

The ¹H-¹³C HETCOR spectrum of **1** shown in Figure 4 allows assignment of the hydride resonances and provides partial assignment of the carbonyl ligand signals. Thus, cross peaks between the hydride peak at δ -17.6 and the unique ¹³C peak near δ 167, which is assigned as the CO ligand on the iridium atom (e), prompts assignment of the former as the resonance for the hydride bridging the Ir-Re edge (H_b). Then the cross peaks between the hydride peak at δ -16.5 due to the hydride ligand bridging the Re-Re edge (H_a) indicate resonances due to CO ligands on the rhenium atoms. The specific assignments of the Re-CO resonances rely on the observation that coupling between a ¹H nucleus and ¹³C or ³¹P nuclei in a cis relationship is larger than that for a trans orientation.³² Therefore, the Re-CO peak labeled d' is assigned on the basis of the cross peak with H_b and the lack of a cross peak with H_a; the CO peak d' is due to a carbonyl in the equatorial plane in a position cis to H_b and trans to H_a (see diagram with Table 3). Further, the cross peak between H_b and the set of peaks near 182.5 ppm suggests the latter contains resonances for CO ligands b' and c', which are also oriented cis to H_b. On this basis a cross peak between the signals due to H_b and d is not expected (d is trans to H_b), but overlap of the b', c', and d signals obviates any conclusion. However, as expected, no cross peak is seen between H_a and its trans oriented carbonyl a'. The ¹³C peaks below 185 ppm are all coupled to H_a, suggesting they are oriented cis to this hydride. The variable-temperature behavior of the ¹³C NMR spectra (see below) provides further support for these assignments.

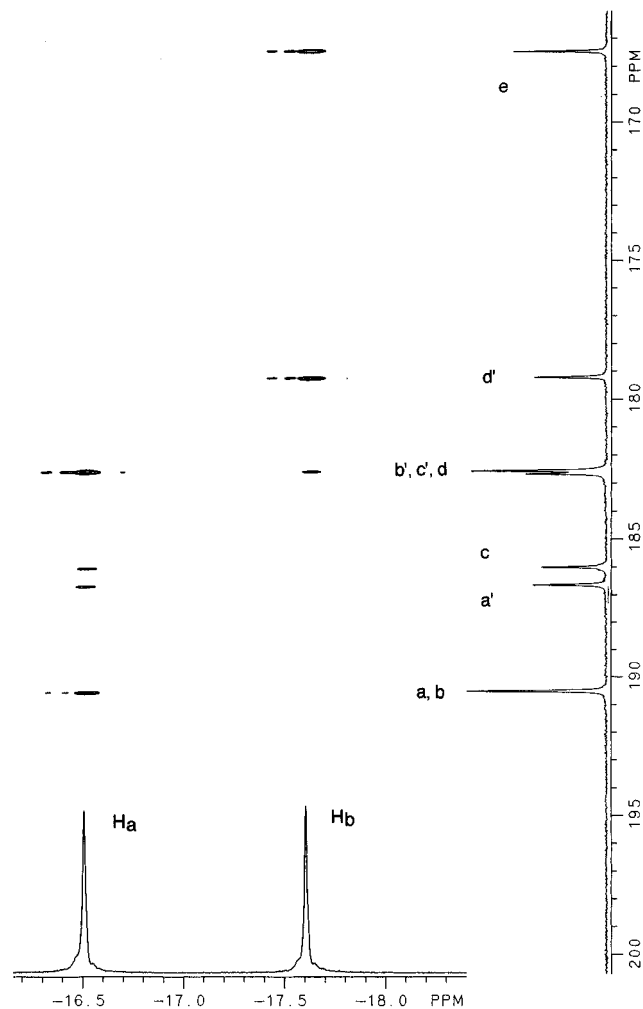


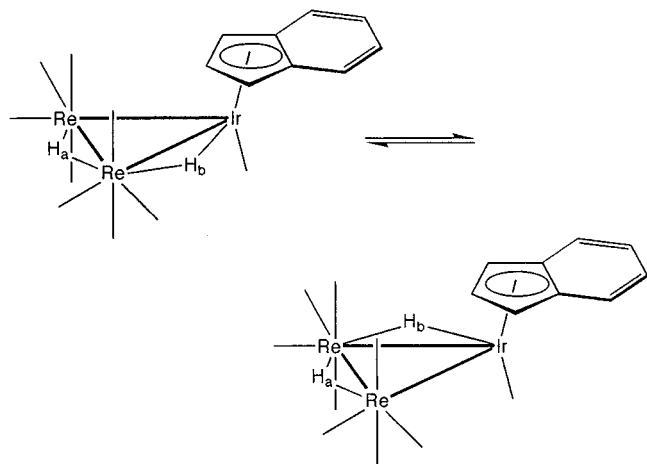
Figure 4. ¹H-¹³C HETCOR spectrum of **1** in CD₂Cl₂ at -80 °C.

Dynamic NMR Behavior of 1. As the sample temperature is raised from -70 °C, the proton signals for H₁ and H₃ of the indenyl ligand broaden and coalesce until at 20 °C only one broad resonance is observed (see Figure 2). In contrast, however, the two hydride signals in the ¹H spectrum (see spectra in the Supporting Information) are invariant over the temperature range explored. Similarly, the peaks between 192 and 179 ppm in the low temperature ¹³C spectrum of **1** broaden, coalesce, and form four broad peaks at 25 °C, but the ¹³C peak at δ 167.5 remains sharp throughout (see Figure 3). The pairs of signals that coalesce can be determined by comparing the chemical shifts of the peaks in the spectrum obtained at 45 °C with the average chemical shift values calculated from the spectrum at -80 °C. For example, the a and a' resonances appear at δ 191.17 and 187.08 at -80 °C, leading to an average value of δ 189.13, which compares to δ 188.71 assigned to the rapid exchange position of these same peaks. The difference in calculated and observed values is $+0.4$ ppm, and this same discrepancy is consistently seen for the other pairs of CO peaks. The same amount of line broadening evidenced by each of the ¹³C peaks in going from -80 to -40 °C implies that a single dynamic process is responsible for the observed signal equilibration.

Taken together the NMR data require a dynamic process that generates an effective mirror plane perpendicular to the IrRe₂ triangle, bisecting the indenyl ligand and passing through the hydride ligand bridging the Re-Re edge. This process causes equilibration of the H₁ and H₃ protons (together with H₄/H₇ and H₅/H₆) on the indenyl ligand as well as the CO ligands on the two rhenium centers as described above. The most likely

(32) (a) Beringhelli, T.; Ciani, G.; D'Alfonso, G.; Freni, M. *J. Organomet. Chem.* **1986**, *311*, C51. (b) Beringhelli, T.; D'Alfonso, G.; Freni, M.; Minoja, A. P. *Inorg. Chem.* **1996**, *35*, 2393.

Scheme 2



mechanism involves migration of hydride H_b between the two Ir–Re edges (see Scheme 2). The free energy of activation, ΔG^\ddagger , for the process causing equilibration of H_1 and H_3 ($\Delta\nu = 323$ Hz) was calculated from the rate constant at the temperature of coalescence (-15°C) by using the equations, $k_c = \pi\Delta\nu(2)^{-1/2} = (k_b T_c/h) \exp[-\Delta G_c^\ddagger/RT_c]$, leading to $\Delta G_c^\ddagger = 11.7(6)$ kcal mol $^{-1}$. The error in ΔG_c^\ddagger was propagated from estimated errors in $\Delta\nu$ and T_c . A similar value of ΔG_c^\ddagger can be estimated from the ^{13}C spectra, since the important parameters are nearly the same ($\Delta\nu$ ca. 300 Hz, T_c ca. 10°C ; see Figure 3).

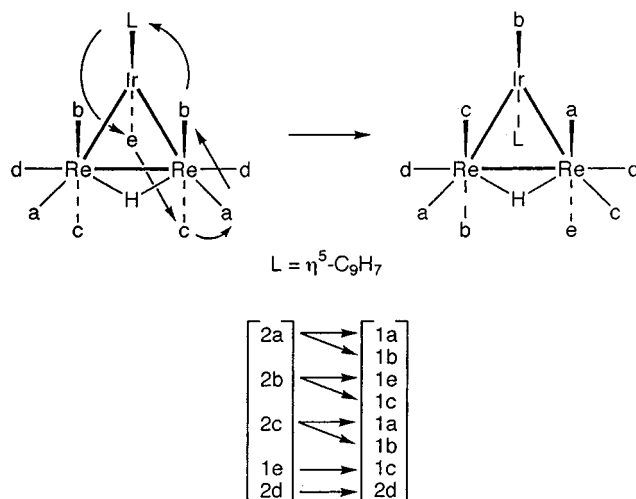
A similar situation was observed for the related cluster $\text{PtRe}_2(\mu\text{-H})_2(\text{CO})_8(\eta^4\text{-C}_8\text{H}_{12})$.⁸ The ^1H NMR peaks for the hydrides bridging the Re–Re and Pt–Re edges were sharp at all temperatures. However, the ^{13}C NMR signals for the carbonyl ligands on the Re atoms, which appeared as three sharp signals in a 2:1:1 ratio at -10°C were observed to broaden and collapse near -88°C . Thus, a dynamic process caused the apparent C_{2v} symmetry at higher temperatures, and a mechanism involving the migration of one hydride ligand between the two Pt–Re edges provided a satisfactory explanation.

Synthesis and Spectroscopic Characterization of 2. One of the bridging hydride ligands in **1** is readily removed by deprotonation. Addition of an ethanolic solution of KOH to a suspension of yellow **1** in ethanol results in an immediate color change to deep red and complete dissolution of remaining solid **1**. The infrared spectrum of this solution is similar to that for **1** except that all the peaks are shifted to lower energy. Addition of excess [PPN]Cl and holding the solution at -20°C results in the precipitation of red needles of [PPN][$\text{IrRe}_2(\mu\text{-H})(\text{CO})_9(\eta^5\text{-C}_9\text{H}_7)$] (**2**). The molecular formula for **2** is supported by mass spectrometry and microanalysis. The deprotonation of $\text{Re}_3(\mu\text{-H})_3(\text{CO})_{12}$ under similar conditions provided $[\text{Re}_3(\mu\text{-H})_2(\text{CO})_{12}]^-$.²³

The ^1H NMR spectrum for **2** shows one hydride resonance at $\delta -17.78$. In the indenyl region only four peaks are observed, consistent with a structure in which the indenyl ligand resides in a symmetric site; in particular H_1 and H_3 are equivalent (see Table 3). No dynamic behavior is observed in the ^1H NMR spectra for **2** between -80 and 20°C ; both the indenyl and the hydride resonances remain sharp, and the line widths are invariant over the same temperature range. These data indicate that deprotonation removes the hydride bridging the Ir–Re edge and the remaining hydride is located on the Re–Re edge, which is bisected by the resulting mirror plane perpendicular to the IrRe_2 triangle.

The $^{13}\text{C}\{^1\text{H}\}$ NMR spectrum of **2** at -60°C is consistent with the discussion above (see Figure 4 and Table 3), with one

Scheme 3



Ir–CO peak (e) and four Re–CO peaks (a–d). The peaks labeled a, b, and c appear as doublets in the uncoupled spectrum, with $J_{\text{HC}} = 2.7, 3.0,$ and 4.0 Hz, respectively. The similar J_{HC} coupling constants for these peaks suggest they are all due to $^2J_{\text{HC}}(\text{cis})$ interactions rather than two $^2J_{\text{HC}}(\text{cis})$ and one $^2J_{\text{HC}}(\text{trans})$.³² Furthermore, as described below, the peak labeled d occupies the equatorial site trans to the $\text{Re}(\mu\text{-H})\text{Re}$ bond.

Dynamic NMR Behavior of 2. As the temperature is raised above -40°C , the ^{13}C NMR spectrum of **2** shows that the a, b, and c Re–CO peaks as well as the Ir–CO peak (e) all broaden, while the Re–CO peak labeled d remains invariant. These data imply the operation of a carbonyl scrambling process that is localized on the Ir–Re edges but does not include carbonyl d, which occupies a site trans to the $\text{Re}(\mu\text{-H})\text{Re}$ bond. The cyclic process shown in Scheme 3 meets these requirements.

Considering one cycle of exchange, the proposed mechanism involves the site exchanges of $e \rightarrow c, c \rightarrow a, a \rightarrow b,$ and $b \rightarrow e$, with the last accompanied by a shift of the indenyl ligand to the other side of the IrRe_2 triangle. Furthermore, this migration of the indenyl ligand causes exchange of the b and c carbonyls ($b \rightarrow c, c \rightarrow b$) on the second rhenium atom but leaves site a at this rhenium center unchanged. Therefore, for each cycle two spins are exchanged out of both the b and c sites, whereas only one spin is exchanged out of the a and the e sites. However, since there are 2C for each of the a, b, and c sites but only 1C for the e site, the net exchange rate constant is k for the b, c, and e sites and $1/2k$ for the a site. Since line broadening is proportional to the first-order rate constant for spins leaving a given site ($k = \pi(\Delta\nu - \Delta\nu_0)$), resonances for sites b, c, and e should broaden faster than that for a. Comparison of the respective line widths among the 2C signals a, b, and c in the spectrum at 0°C in Figure 5 clearly shows that the peaks assigned to b and c are broader than that for a; the situation for the 1C signal e is less clear. Nevertheless, the selective line broadening observed for b/c vs a provides strong support for the proposed mechanism. The line widths of the b and c peaks are estimated at ca. 20 Hz in the spectrum at 0°C and are ca. 3 Hz in the limiting spectrum at -60°C . Therefore, at 273 K, $k = \pi(20 - 3) = 53 \text{ s}^{-1}$, which leads via the Eyring equation to $\Delta G^\ddagger = 13.8(5)$ kcal mol $^{-1}$, with errors propagated from estimated errors in k and T .

An analogous cyclic scrambling mechanism has been deduced for $\text{IrOs}_2(\text{CO})_9(\eta^5\text{-C}_5\text{H}_5)$.³³ At -48°C the ^{13}C NMR spectrum of this cluster shows five sharp carbonyl peaks, consistent with

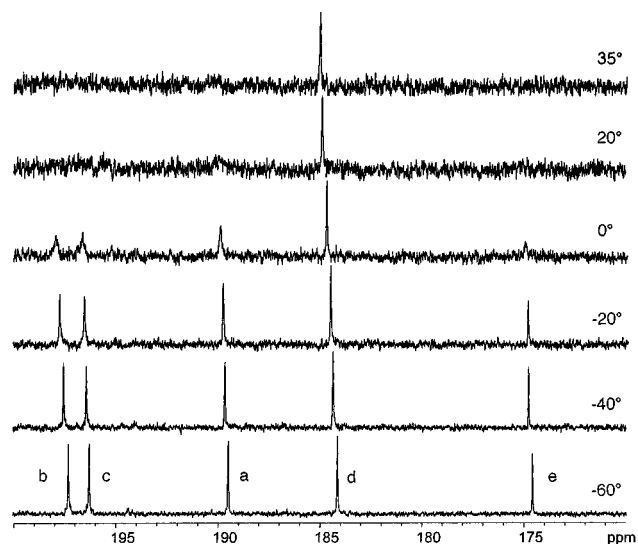


Figure 5. Carbon-13 NMR spectra (carbonyl region) of **2** in CD₂Cl₂ at temperatures between 35 and -60 °C.

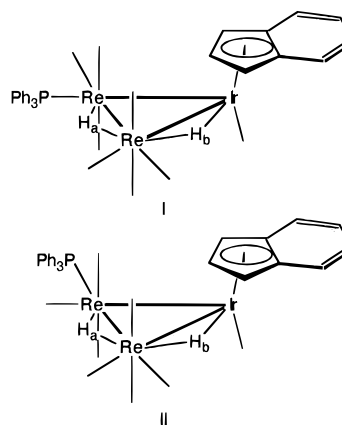
the expected C_s symmetric structure. At 7 °C only four of these peaks have collapsed, while one sharp singlet remains. Simulation of the spectrum at -10 °C gave $k = 9(1) \text{ s}^{-1}$ and correspondingly $\Delta G^\ddagger = 14.2(3) \text{ kcal mol}^{-1}$, which is remarkably close to the value we determine for **2**. Interestingly, the analog IrOs₂(CO)₉(η⁵-C₅Me₅) appears to undergo the same process with a much lower activation barrier, $\Delta G^\ddagger = 7.4(2) \text{ kcal mol}^{-1}$ at -116 °C, consistent with stabilization of a carbonyl bridged intermediate configuration by the more basic Cp* ligand. Note that in neither of these cases nor in the case of **2** does a process involving rotation of the Ir(CO)(η⁵-L) vertex relative to the remaining M₂ unit correlate with the spectral changes observed. However, an interesting example of such metal vertex rotation in a Re₃ cluster has been reported recently.³⁴

Reaction of 1 with PPh₃ and Formation of 3. The reaction of **1** with PPh₃ is neither facile nor clean. From the reaction in hexane at reflux a significant amount of unreacted **1** was recovered, and a product subsequently characterized as IrRe₂(μ-H)₂(CO)₈(PPh₃)(η⁵-C₉H₇) (**3**) was isolated in pure form after careful chromatography. Other, minor products were produced, as observed by TLC, but they were not isolated in pure form and were not characterized. Infrared spectra obtained during the course of the reaction suggested the concurrent formation of ReH(CO)₄(PPh₃).¹⁵

The ¹H NMR spectrum for **3** (see Table 3) shows the indenyl H₁ and H₃ protons are inequivalent; thus, the indenyl ligand resides in an asymmetric site. In the hydride region, a doublet at $\delta -15.19$ ($J_{\text{PH}} = 16.4 \text{ Hz}$) and a singlet at $\delta -17.12$ appear. No change in line width is observed for either the indenyl or the hydride resonances in spectra obtained between 25 and -80 °C. The ³¹P{¹H} spectrum contains a single peak at +14.4 ppm. The ¹³C{¹H} NMR of a ¹³CO-enriched sample of **3** clearly indicates that the phosphine ligand is not on the iridium atom (see Table 3 and the Supporting Information). A singlet is observed at $\delta 168.4$ for the Ir-CO ligand. In addition three doublets and four singlets are observed between 193 and 182 ppm for the Re-CO ligands. The coupling constants for the three doublets are very similar ($J_{\text{PC}} = 6.6, 7.9, \text{ and } 8.2 \text{ Hz}$), which suggests an equatorial site for the phosphine ligand, i.e.,

a position cis to the three remaining CO ligands on the substituted rhenium center.

The NMR data for **3** are consistent with structures I and II, which have the phosphine ligand on the rhenium atom that is



not bonded to H_b. If the phosphine ligand were bound to the rhenium atom involved in the Re(μ-H_b)Ir bridge, some coupling between H_b and the phosphorus nucleus would be expected. However, a number of studies on phosphine-substituted hydridorhenium carbonyl cluster compounds by Beringhelli, D'Alfonso, and co-workers^{9,32} have demonstrated that ²J_{PH(cis)} is significantly larger than ²J_{PH(trans)}. On the basis of these observations, the relatively large value of $J_{\text{PH}} = 16.4 \text{ Hz}$ observed for **3** is more consistent with structure I, containing an equatorially bound phosphine ligand in the position trans to the unsupported Ir-Re bond and cis to the Re(μ-H_a)Re moiety, than with structure II, for which a smaller coupling, ²J_{PH(trans)}, would be expected.

When the reaction of **1** with PPh₃ was repeated with 2 equiv of the entering ligand, more **1** was consumed, but more ReH(CO)₄(PPh₃) was observed by infrared spectroscopy, and the yield of **3** was unchanged. Isolation of **3** as the only significant substitution product from **1** is at first glance not expected. A product containing the phosphine ligand on the iridium atom would appear to be more consistent with the high reactivity observed for mononuclear indenyl compounds in associative substitution reactions.^{1,12} However, we have observed that reactions of the trinuclear indenyl cluster Ir₃(μ-CO)₃(η⁵-C₉H₇)₃ with CO² or PPh₃³⁵ lead immediately at room temperature to the mononuclear cluster fragmentation products, Ir(CO)(L)(η⁵-C₉H₇) (L = CO, PPh₃). Therefore, associative attack of PPh₃ at the iridium center in **1** may lead to displacement of the Re₂(μ-H)₂(CO)₈ pseudoolefin fragment rather than CO, with consequent formation of Ir(CO)(PPh₃)(η⁵-C₉H₇). The presence of Ir(CO)(PPh₃)(η⁵-C₉H₇) was not detected during the reaction; however, this compound has been found to react with excess PPh₃ at room temperature, leading to other products.³⁵ Subsequent reaction of Re₂(μ-H)₂(CO)₈ with PPh₃ would lead to ReH(CO)₄(PPh₃), as observed previously.^{13,36}

Summary

The reaction of Re₂(μ-H)₂(CO)₈ with Ir(CO)(η²-C₈H₁₄)(η⁵-C₉H₇) provides the trinuclear cluster, IrRe₂(μ-H)₂(CO)₉(η⁵-C₉H₇), **1**, in high yield. The X-ray structure and NMR spectroscopy of **1** at low temperatures are consistent with structure having one hydride ligand bridging the Re-Re edge and the second hydride bridging one Ir-Re edge. A dynamic

(33) Riesen, A.; Einstein, F. W. B.; Ma, A. K.; Pomeroy, R. K.; Shipley, J. A. *Organometallics* **1991**, *10*, 3629.

(34) Beringhelli, T.; D'Alfonso, G.; Freni, M.; Panigati, M. *Organometallics* **1997**, *16*, 2719.

(35) Comstock, M. C. Ph.D. Thesis, University of Illinois, 1996.

(36) Prest, D. W.; Mays, M. J.; Raithby, P. R. *J. Chem. Soc., Dalton Trans.* **1982**, 2021.

process involving the migration of one hydride between the two Ir–Re edges has been revealed by variable-temperature ^1H and ^{13}C NMR spectroscopy. Deprotonation of **1** with KOH/EtOH and addition of [PPN][Cl] provides [PPN][IrRe₂(μ -H)(CO)₉(η^5 -C₉H₇)], **2**. Proton and carbon NMR spectra for **2** indicate that the remaining hydride bridges the Re–Re edge, and variable-temperature ^{13}C NMR experiments are consistent with a cyclic carbonyl scrambling process localized on the Ir–Re edges. The reaction of **1** with PPh₃ leads to the carbonyl ligand substitution product, IrRe₂(μ -H)₂(CO)₈(PPh₃)(η^5 -C₉H₇), **3**, as well as to cluster fragmentation. On the basis of ^1H and ^{13}C NMR spectroscopy, the phosphine ligand in **3** is bound to a rhenium atom in an equatorial site, trans to the unbridged Ir–Re bond.

Acknowledgment. This research was supported by a grant from the National Science Foundation (CHE94-14217). M.C.C.

thanks the Department of Chemistry for a fellowship funded by the Lubrizol Corp. We thank Drs. Vera Mainz and Scott T. Massey for help with the HETCOR experiment for **1** and the variable-temperature ^{13}C NMR experiments for **2**, respectively.

Supporting Information Available: Complete tables of atom coordinates, distances and angles, and anisotropic displacement parameters, for **1**, as well as ^1H NMR spectra of **1** in the hydride region between 20 and -70 °C, and the ^{13}C NMR spectrum of **3** (6 pages). Ordering information and instructions for Internet access are given on any current masthead page.

IC960990I